

Control of a Hydraulic Excavator Manipulator

Éverton Lins de Oliveira ¹, Décio Crisol Donha ²

^{1,2} Mechanical Engineering Department, Polytechnic School, University of São Paulo, Av. Prof. Mello Moraes, 2231, São Paulo-SP, Brazil, ev_lins@usp.br, decdonha@usp.br

Abstract: Hydraulic excavators are versatile machines used in a wide range of operations such as digging, removal of debris, transportation of cargo and earthmoving in general. Operating a hydraulic excavator in certain environments is a difficult and dangerous task, especially in hazardous environments subject to natural disturbances or inadequate health conditions for human work. Because of these conditions, the automation of excavators or its components has been the subject of many studies in last years. In this paper, a control system for the manipulator of a mini-excavator is synthesized. The control is based on a reduced mathematical model proposed by the authors to represent all the manipulator dynamics. The work includes results from the controller tests by means of computational simulation with a complete reference model. Results are discussed and evaluated and suggestions for future work are enclosed.

Keywords: hydraulic excavator, hydraulic manipulator, excavator control, manipulator control.

INTRODUCTION

Hydraulic excavators are versatile machines used in various types of operations, such as digging, removing debris, cargo, ground and earthworks in general. Operating a hydraulic excavator in certain environments is a difficult task, especially when it comes to dangerous environments subject to natural disturbances or inadequate health conditions for human work. In last years, the excavators' automation has been the subject of many studies, seeking high efficiency and improved safety. Some papers in the literature focus only on the control of the manipulator mechanics (Koivo et al., 1996; Hoan et al., 2011). However, the control of the whole manipulator (considering its mechanic and hydraulic) is essential in the experimental application (Nguyen, 2000; He et al., 2006). Therefore, to synthesize a suitable control system for the manipulator of a hydraulic excavator, it is necessary to develop a controller algorithm to handle all the manipulator dynamics.

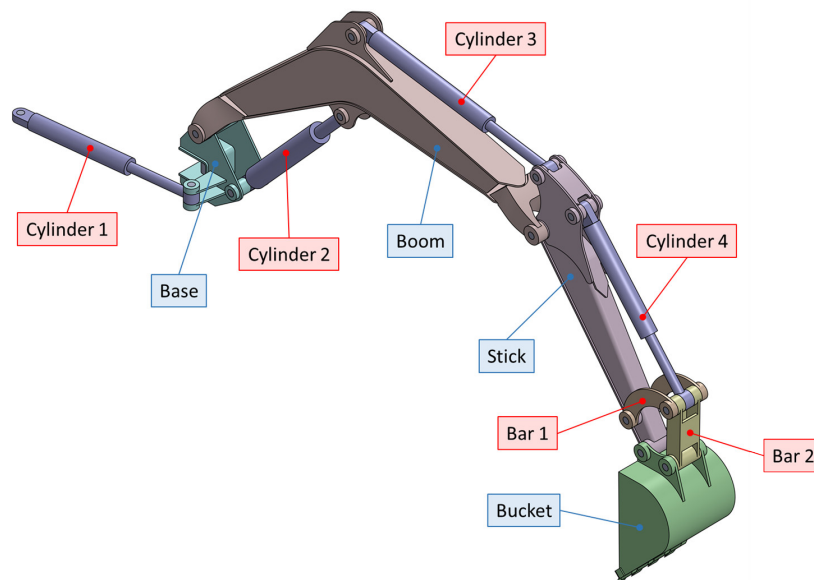


Figure 1 – Manipulator studied and its main components.

In this work, to enable the automation of the equipment shown in Fig. 1, a control system is developed considering all the dynamics of its manipulator. For this, first, the reference dynamic model of the manipulator is presented. This model is divided into two interconnected subsystems, a mechanical and a hydraulic one. To controller synthesize, the reduced models of these subsystems are introduced. The control law for the mechanical subsystem is synthesized with the sliding mode control (SMC) technic and considering a disturbance observer (also based on the SMC). The hydraulic subsystem control law is composed of a feedback linearization with an H-infinity compensation term. In the sequence, to obtain the complete controller of the manipulator, the controls laws are coupled through the cascade structure. The

developed controller is tested through numerical simulation in the MATLAB/Simulink® environment. This simulation is performed with the reference model in a complete operation, involving digging and dump tasks. Finally, the results from the simulation are analyzed and suggestions for future works are enclosed.

REFERENCE MODEL

Due to the manipulator’s architecture (hydraulic actuated mechanism), its model can be divided into three parts: 1) mechanical subsystem model, 2) hydraulic subsystem model and 3) manipulator coupled model. In sequence, each part of the reference model will be specified.

Mechanical subsystem model

The mechanical subsystem model was derived with the following assumptions: 1) the links of the manipulator (base, boom, stick, bucket, cylinders and bars) are rigid bodies, and 2) only the friction on the cylinders is relevant. With these assumptions, the mechanical subsystem model can be written as:

$$\ddot{\mathbf{q}} = \mathbf{M}^{-1} \left(\mathbf{J}^T \mathbf{F}_h - \mathbf{C}\dot{\mathbf{q}} - \mathbf{J}^T \mathbf{F}_f - \mathbf{G} - \boldsymbol{\tau}_{\text{task}} \right), \quad (1)$$

where $\mathbf{q} \in \mathfrak{R}^4$ is the vector of generalized coordinates with $\dot{\mathbf{q}} \in \mathfrak{R}^4$ and $\ddot{\mathbf{q}} \in \mathfrak{R}^4$ as its first and second derivative with respect to time, respectively, $\mathbf{M} \in \mathfrak{R}^{4 \times 4}$ is the matrix of inertia, $\mathbf{C} \in \mathfrak{R}^{4 \times 4}$ is the matrix of Coriolis and centripetal efforts, $\mathbf{F}_f \in \mathfrak{R}^4$ is the vector of friction forces of the cylinders, $\mathbf{G} \in \mathfrak{R}^4$ is the vector of gravity torques, $\boldsymbol{\tau}_{\text{task}} \in \mathfrak{R}^4$ is the vector of task torques (generalized efforts from digging and dump), $\mathbf{J} \in \mathfrak{R}^{4 \times 4}$ is the Jacobian matrix, which relates joints space with cylinders space and $\mathbf{F}_h \in \mathfrak{R}^4$ is the vector of hydraulic forces.

Hydraulic subsystem model

The model presented here is based on the study of the hydraulic servo system shown in Fig. 2. This system consists of a double action differential cylinder controlled by a 4/3-way proportional directional control valve.

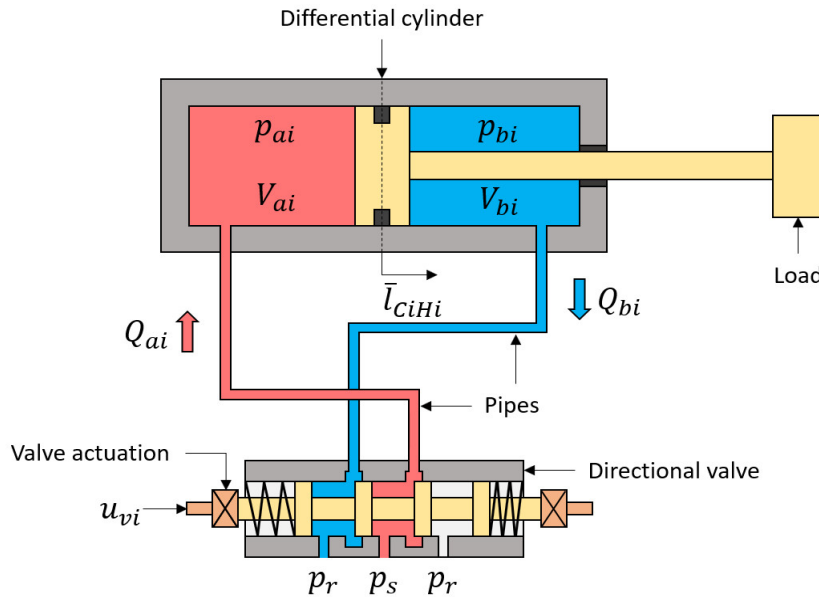


Figure 2 – Hydraulic drive subsystem of the manipulator.

The hydraulic subsystem model was derived with the following assumptions: 1) the supply unit provides constant pressure and flow; 2) the valve internal leakage flow is not significant; 3) the valve dead zone is negligible; 4) the flow regime through the valve orifices is turbulent; 5) the dynamics of the pipelines is insignificant, therefore, these can be modeled as inefficient volumes, and 6) the leakage flow between cylinders and environment is not relevant.

The hydraulic subsystem model will be divided into the followings sections: 1) electromechanical drive model, 2) chambers’ pressures model and 3) hydraulic force model.

Electromechanical drive model

As shown in Valdiero (2005), the dynamic model of the electromechanical drive is composed by a first-order linear model to describe the dynamics of the valve drive force and by a second-order linear model to describe the dynamics of the mechanical part (spool) of the valve. However, depending on the valve’s manufacturing characteristics, its motion

and electromechanical actuation can be described together by a second-order linear model (Valdiero, 2005). Thus, in this work, the same model is adapted to the multivariable case, as follows:

$$\ddot{\mathbf{x}}_v = \mathbf{K}_e \boldsymbol{\Omega}_v^2 \mathbf{u}_v - \boldsymbol{\Omega}_v^2 \mathbf{x}_v - 2\mathbf{Z}_v \boldsymbol{\Omega}_v \dot{\mathbf{x}}_v, \quad (2)$$

where $\mathbf{x}_v \in \mathfrak{R}^4$ is the vector of control displacements with $\dot{\mathbf{x}}_v \in \mathfrak{R}^4$ and $\ddot{\mathbf{x}}_v \in \mathfrak{R}^4$ as its first and second time derivative, in this order; $\mathbf{u}_v \in \mathfrak{R}^4$ is the vector of drive voltages and the terms $\mathbf{K}_e \in \mathfrak{R}^{4 \times 4}$, $\boldsymbol{\Omega}_v \in \mathfrak{R}^{4 \times 4}$ and $\mathbf{Z}_v \in \mathfrak{R}^{4 \times 4}$ are matrices that represent the gains of the electromechanical drive, natural frequencies and damping coefficients, respectively.

Chambers' pressures model

Applying the continuity equation in the cylinders' chambers as described in Merrit (1967), one obtains the dynamic model of the pressures developed in the chambers as follows (Santos, 2001):

$$\dot{\mathbf{p}}_a = \mathbf{E}_a \mathbf{x}_v - \mathbf{F}_a \mathbf{J}^T \dot{\mathbf{q}} - \mathbf{D}_a \mathbf{C}_{in} \Delta \mathbf{p}, \quad (3)$$

$$\dot{\mathbf{p}}_b = \mathbf{F}_b \mathbf{J}^T \dot{\mathbf{q}} + \mathbf{D}_b \mathbf{C}_{in} \Delta \mathbf{p} - \mathbf{E}_b \mathbf{x}_v, \quad (4)$$

where $\mathbf{E}_{a,b} \in \mathfrak{R}^{4 \times 4}$, $\mathbf{F}_{a,b} \in \mathfrak{R}^{4 \times 4}$ and $\mathbf{D}_{a,b} \in \mathfrak{R}^{4 \times 4}$ (the subscripts a and b are referent to the cylinders' chambers) are matrices that take into account the dynamic effects (fluid compressibility, volume change of the cylinders' chambers due to the manipulator's motion, valves' flow rate and leakage flow between the cylinders' chambers); $\mathbf{C}_{in} \in \mathfrak{R}^{4 \times 4}$ is the matrix of leakage coefficients, $\mathbf{p}_{a,b} \in \mathfrak{R}^4$ are the vectors of pressures in the chambers and $\Delta \mathbf{p} \in \mathfrak{R}^4$ is the vector of pressure difference between the chambers.

Hydraulic force model

The hydraulic force vector is derived by the static equilibrium analysis of the cylinders (considering the net forces generated by the pressures in the cylinders' chambers) as follows (Santos, 2001):

$$\mathbf{F}_h = \mathbf{A}_a \mathbf{p}_a - \mathbf{A}_b \mathbf{p}_b, \quad (5)$$

with $\mathbf{A}_{a,b} \in \mathfrak{R}^{4 \times 4}$ as the matrices of cross-section areas of the cylinders (bore- a and rod- b).

Manipulator coupled model

The coupled model of the manipulator is obtained putting the mathematical model in the form of state space through the assigning of state variables, as shown below:

$$\dot{\mathbf{x}} = \mathbf{f}(\mathbf{x}, \mathbf{u}), \quad (6)$$

where $\mathbf{x} = [\mathbf{x}_1^T, \dots, \mathbf{x}_6^T]^T$ is the state vector, with $\mathbf{x}_1 = \mathbf{q} \in \mathfrak{R}^4$, $\mathbf{x}_2 = \dot{\mathbf{q}} \in \mathfrak{R}^4$, $\mathbf{x}_3 = \mathbf{p}_a \in \mathfrak{R}^4$, $\mathbf{x}_4 = \mathbf{p}_b \in \mathfrak{R}^4$, $\mathbf{x}_5 = \mathbf{x}_v \in \mathfrak{R}^4$ and $\mathbf{x}_6 = \dot{\mathbf{x}}_v \in \mathfrak{R}^4$ as the states; $\mathbf{u} = \mathbf{u}_v \in \mathfrak{R}^4$ is the vector of control signals and $\mathbf{f} \in \mathfrak{R}^{24}$ is the vector of nonlinear functions, that is given by:

$$\mathbf{f}(\mathbf{x}, \mathbf{u}) = \begin{bmatrix} \mathbf{x}_2 \\ \mathbf{M}^{-1} \left(\mathbf{J}^T \mathbf{F}_h - \mathbf{C} \mathbf{x}_2 - \mathbf{J}^T \mathbf{F}_f - \mathbf{G} - \boldsymbol{\tau}_{\text{task}} \right) \\ \mathbf{E}_a \mathbf{x}_5 - \mathbf{F}_a \mathbf{J}^T \mathbf{x}_2 - \mathbf{D}_a \mathbf{C}_{in} \Delta \mathbf{p} \\ \mathbf{F}_b \mathbf{J}^T \mathbf{x}_2 + \mathbf{D}_b \mathbf{C}_{in} \Delta \mathbf{p} - \mathbf{E}_b \mathbf{x}_5 \\ \mathbf{x}_6 \\ \mathbf{K}_e \boldsymbol{\Omega}_v^2 \mathbf{u} - \boldsymbol{\Omega}_v^2 \mathbf{x}_5 - 2\mathbf{Z}_v \boldsymbol{\Omega}_v \mathbf{x}_6 \end{bmatrix}. \quad (7)$$

The reference model presented here is used in the simulation of the controller.

CASCADE CONTROL

The cascade control structure applied in the manipulator consist of two terms. The first one is the control law of the mechanical subsystem that generates the vector of desired hydraulic forces ($\mathbf{F}_{hd} \in \mathfrak{R}^4$) relative to the mechanical efforts required to track the desired path (x_d, y_d, z_d) as close as possible. The second term is the control law of the hydraulic subsystem that generates the vector of control signals ($\mathbf{u}_v \in \mathfrak{R}^4$) that makes the generated hydraulic forces ($\mathbf{F}_h \in \mathfrak{R}^4$) track the desired ones. In Figure 3 is shown the block diagram of the cascade control applied to the manipulator.

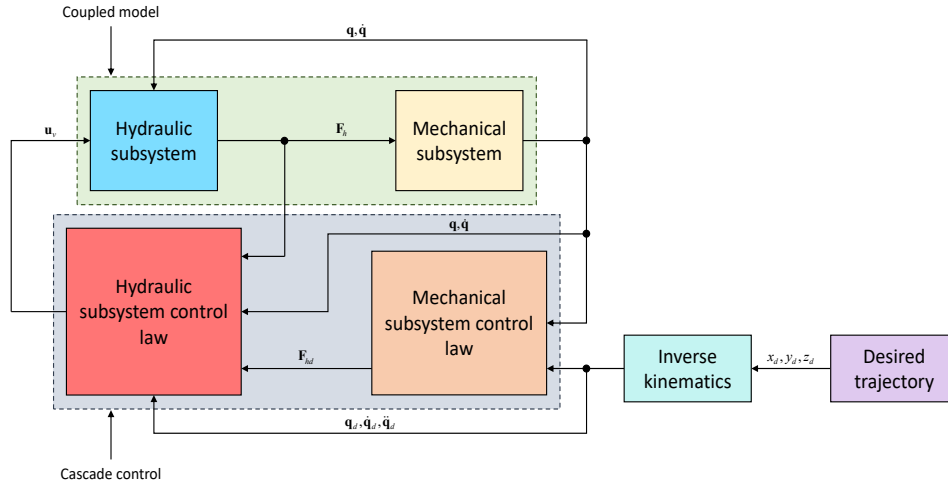


Figure 3 – Block diagram of the cascade control.

A real operating environment is highly dynamic and uncertain. Thus, to synthesize a robust control algorithm to the manipulator, the presence of disturbances and uncertainties must be considered in the synthesis of both control laws. In the following sections, the control laws of the subsystems are presented.

Mechanical subsystem controller

The control law of the mechanical subsystem will be divided into the followings sections: 1) mechanical subsystem reduced model, 2) sliding mode control and 3) sliding mode disturbance observer (SMDO).

Mechanical subsystem reduced model

The matrices of the mechanical subsystem dynamic model can be rewritten in terms of the contributions of the main links (base, boom, stick and bucket), cylinders and bars, as shown below:

$$\ddot{\mathbf{q}} = (\mathbf{M}_l + \mathbf{M}_c + \mathbf{M}_b)^{-1} \left[\mathbf{J}^T \mathbf{F}_h - (\mathbf{C}_l + \mathbf{C}_c + \mathbf{C}_b) \dot{\mathbf{q}} - \mathbf{J}^T \mathbf{F}_f - (\mathbf{G}_l + \mathbf{G}_c + \mathbf{G}_b) - \boldsymbol{\tau}_{\text{task}} \right], \quad (8)$$

where the indices l , c and b are referring to the contributions of the main links, cylinders and bars, respectively. The reduced model of the mechanical subsystem is derived through the following assumptions: 1) the manipulator's motion is slow, 2) the gravity torques are the main contributions to the dynamics in free space motion, and 3) the bars are not relevant in the dynamics. Thus, from Eq. (8), the reduced model can be written as:

$$\ddot{\mathbf{q}} = (\mathbf{M}_l + \mathbf{M}_c)^{-1} \left[\mathbf{J}^T \mathbf{F}_h - (\mathbf{G}_l + \mathbf{G}_c) - \boldsymbol{\tau}_d \right], \quad (9)$$

where $\boldsymbol{\tau}_d \in \mathfrak{R}^4$ is the vector of disturbance torques, that is given by:

$$\boldsymbol{\tau}_d = \mathbf{M}_b \ddot{\mathbf{q}} + \mathbf{C} \dot{\mathbf{q}} + \mathbf{J}^T \mathbf{F}_f + \mathbf{G}_b + \boldsymbol{\tau}_{\text{task}}. \quad (10)$$

It is also assumed that task efforts and friction torques are much higher than the neglected terms of the model, hence, $\|\mathbf{J}^T \mathbf{F}_f + \boldsymbol{\tau}_{\text{task}}\|_2 \gg \|\mathbf{M}_b \ddot{\mathbf{q}} + \mathbf{C} \dot{\mathbf{q}} + \mathbf{G}_b\|_2$, thus, the vector of disturbance torques will be: $\boldsymbol{\tau}_d \cong \mathbf{J}^T \mathbf{F}_f + \boldsymbol{\tau}_{\text{task}}$. Therefore, the reduced model of the mechanical subsystem can be rewritten as shown below:

$$\ddot{\mathbf{q}} = \hat{\mathbf{M}}^{-1} (\mathbf{F}_h - \hat{\mathbf{G}} - \hat{\mathbf{F}}_d), \quad (11)$$

with $\hat{\mathbf{M}} = \mathbf{J}^{-T} (\mathbf{M}_l + \mathbf{M}_c)$, $\hat{\mathbf{G}} = \mathbf{J}^{-T} (\mathbf{G}_l + \mathbf{G}_c)$ and $\hat{\mathbf{F}}_d = \hat{\mathbf{F}}_f + \mathbf{J}^{-T} \hat{\boldsymbol{\tau}}_{\text{task}}$. The symbol “ $\hat{}$ ” is used on the matrices of the Eq. (11) to show that model can be interpreted as an estimative of the complete one given by Eq. (8).

Sliding mode control

The objective of the SMC is to make the mechanical subsystem track a desired trajectory even in the presence of model uncertainties and disturbances. For this purpose, the vector of tracking errors is written as:

$$\boldsymbol{\varepsilon} = \begin{bmatrix} \tilde{\mathbf{q}} \\ \dot{\tilde{\mathbf{q}}} \end{bmatrix} = \begin{bmatrix} \mathbf{q} - \mathbf{q}_d \\ \dot{\mathbf{q}} - \dot{\mathbf{q}}_d \end{bmatrix}, \quad (12)$$

where $\tilde{\mathbf{q}} \in \mathfrak{R}^4$ is the vector of tracking errors of joint displacements, $\dot{\tilde{\mathbf{q}}} \in \mathfrak{R}^4$ is the vector of tracking errors of joint velocities, $\mathbf{q}_d \in \mathfrak{R}^4$ is the vector of desired joint displacements and $\dot{\mathbf{q}}_d \in \mathfrak{R}^4$ is its first time derivative.

Considering the SMC theory as presented by Slotine and Li (1991) and introducing the matrix $\mathbf{N} \in \mathfrak{R}^{4 \times 8}$, hence, the switching function can be written as:

$$\mathbf{s} = \mathbf{N}\boldsymbol{\varepsilon} = \underbrace{\begin{bmatrix} \boldsymbol{\Lambda} & \mathbf{I} \\ & \end{bmatrix}}_{\mathbf{N}} \begin{bmatrix} \tilde{\mathbf{q}} \\ \dot{\tilde{\mathbf{q}}} \end{bmatrix} = \boldsymbol{\Lambda}\tilde{\mathbf{q}} + \dot{\tilde{\mathbf{q}}}, \quad (13)$$

with $\boldsymbol{\Lambda} = \text{diag}[\lambda_1, \dots, \lambda_4]$, where $\lambda_i > 0$, as the gain matrix related to the system bandwidth (Slotine and Li, 1991).

The reaching law, considering the inclusion of a proportional rate term that makes the states convergence faster, is given by:

$$\dot{\mathbf{s}} = -\mathbf{Z}\text{sign}(\mathbf{s}) - \mathbf{K}\mathbf{s}, \quad (14)$$

where $\mathbf{Z} = \text{diag}[z_1, \dots, z_4]$, with $z_i > 0$, are the matrix of sliding mode gains, and $\mathbf{K} = \text{diag}[k_1, \dots, k_4]$, with $k_i > 0$, are the matrix of proportional rate gains.

Differentiating the switching function with respect to time and substituting Eq. (11) into the result, one obtains:

$$\dot{\mathbf{s}} = \boldsymbol{\Lambda}\dot{\tilde{\mathbf{q}}} + \ddot{\tilde{\mathbf{q}}} = \boldsymbol{\Lambda}\dot{\tilde{\mathbf{q}}} + \ddot{\tilde{\mathbf{q}}} - \ddot{\mathbf{q}}_d = \boldsymbol{\Lambda}\dot{\tilde{\mathbf{q}}} + \hat{\mathbf{M}}^{-1}(\mathbf{F}_h - \hat{\mathbf{G}} - \hat{\mathbf{F}}_d) - \ddot{\mathbf{q}}_d. \quad (15)$$

Thus, with the Eqs. (14) and (15), the control law of the mechanical subsystem can be written as:

$$\mathbf{F}_h = \hat{\mathbf{M}}[\ddot{\mathbf{q}}_r - \mathbf{Z}\text{sign}(\mathbf{s}) - \mathbf{K}\mathbf{s}] + \hat{\mathbf{G}} + \hat{\mathbf{F}}_d, \quad (16)$$

where $\ddot{\mathbf{q}}_r \in \mathfrak{R}^4$ is the vector of reference acceleration, that is given by: $\ddot{\mathbf{q}}_r = \ddot{\mathbf{q}}_d - \boldsymbol{\Lambda}\dot{\tilde{\mathbf{q}}}$.

Sliding mode disturbance observer

The SMDO synthesized is based on the one proposed by Nguyen (2000). Here, the SMDO is established through the estimation of the joint velocities, as shown below:

$$\dot{\hat{\boldsymbol{\omega}}} = \hat{\mathbf{M}}^{-1}(\mathbf{F}_h - \hat{\mathbf{G}}) + \hat{\boldsymbol{\Phi}} - \mathbf{L}\tilde{\boldsymbol{\omega}}, \quad (17)$$

where $\hat{\boldsymbol{\omega}} \in \mathfrak{R}^4$ is the vector of estimated joint velocities, $\hat{\boldsymbol{\Phi}} \in \mathfrak{R}^4$ is the vector of the estimated dynamics and $\mathbf{L}\tilde{\boldsymbol{\omega}} \in \mathfrak{R}^4$ is a linear feedback term that accelerates the converge of the estimated velocities, with $\mathbf{L} = \text{diag}[l_1, \dots, l_4]$ as the gain matrix, where $l_i > 0$, and $\tilde{\boldsymbol{\omega}} \in \mathfrak{R}^4$ as the vector of estimation errors that is calculated as: $\tilde{\boldsymbol{\omega}} = \hat{\boldsymbol{\omega}} - \dot{\mathbf{q}}$.

The adaptation law is given by (Nguyen, 2000):

$$\dot{\hat{\boldsymbol{\Phi}}} = -\boldsymbol{\Gamma}\text{sign}(\tilde{\boldsymbol{\omega}}), \quad (18)$$

with $\boldsymbol{\Gamma} = \text{diag}[\gamma_1, \dots, \gamma_4]$, where $\gamma_i > 0$, as the gain matrix of the adaptation law. If the estimated velocities converge in finite time, so, $\tilde{\boldsymbol{\omega}} \rightarrow \mathbf{0}$ for $t < \infty$ and $\dot{\hat{\boldsymbol{\Phi}}} \rightarrow -\hat{\mathbf{M}}^{-1}(\mathbf{J}^{-T}\mathbf{M}_b\dot{\tilde{\mathbf{q}}} + \mathbf{J}^{-T}\mathbf{C}\dot{\mathbf{q}} + \mathbf{F}_f + \mathbf{J}^{-T}\mathbf{G}_b + \mathbf{J}^{-T}\boldsymbol{\tau}_{\text{task}})$. Therefore, the vector of estimated disturbances shall be expressed by: $\hat{\mathbf{F}}_d = -\hat{\mathbf{M}}\hat{\boldsymbol{\Phi}}$.

Hydraulic subsystem controller

The control law of the hydraulic subsystem is divided into the followings sections: 1) hydraulic subsystem reduced model, 2) feedback linearization and 3) H-infinity control.

Hydraulic subsystem reduced model

In de Oliveira and Donha (2018) was proposed a reduced model for the hydraulic subsystem of a mini-excavator. This model is based on the relationship between hydraulic force and load pressure. To its derivation the valves dynamics and the leakage flow between cylinders' chambers were considered negligible. In order to include the leakage flow in this representation, the following model of the hydraulic force is proposed (for a mechanism of serial architecture):

$$\dot{\mathbf{F}}_h = \mathbf{A}_a\mathbf{E}_l\mathbf{u}_v - \mathbf{A}_a\mathbf{F}_l\mathbf{J}^T\dot{\mathbf{q}} - \mathbf{A}_a\mathbf{D}_l\mathbf{C}_{in}\Delta\mathbf{p}, \quad (19)$$

where $\mathbf{E}_l \in \mathfrak{R}^{4 \times 4}$, $\mathbf{F}_l \in \mathfrak{R}^{4 \times 4}$ and $\mathbf{D}_l \in \mathfrak{R}^{4 \times 4}$ are the matrices of the reduced model that take into account the dynamic effects (fluid compressibility, change in the volume, valves' flow rate and leakage flow between cylinders' chambers).

Feedback linearization

The serial architecture of the manipulator already makes the hydraulic subsystem model uncoupled in relation to its states (hydraulic forces). Thus, the feedback linearization technique can be used in the hydraulic subsystem control law to compensate for the nonlinearities of its model. Hence, considering the reduced model of the hydraulic subsystem and the feedback linearization technique as presented by Slotine and Li (1991), the proposed control law for the hydraulic subsystem can be written as:

$$\mathbf{u}_v = (\mathbf{A}_a \hat{\mathbf{E}}_l)^{-1} (\mathbf{v} + \mathbf{A}_a \hat{\mathbf{F}}_l \mathbf{J}^T \dot{\mathbf{q}}), \quad (20)$$

where $\mathbf{v} \in \mathfrak{R}^4$ is the linear feedback term that will be presented in the next section. The estimated terms in Eq. (20) are due to the assumption that the bulk modulus is constant, even though it depends on the pressure, temperature and the quantity of air mixed in the hydraulic fluid. The leakage flow is not considered in the control law because it is difficult to determine without experiments. Therefore, the linear feedback term must be able to handle this modeling error.

H-infinity control

As shown in Fales (2004), after the feedback linearization the hydraulic subsystem model can be treated as a linear model. Thus, the linear model for each actuator obtained with the feedback linearization made with Eqs. (20) and (19) can be expressed by the following transfer function (TF) subject to uncertain parameters:

$$F_h(s) = \frac{\varphi_l}{s + \psi_l} v(s) \Rightarrow G_{F_h}(s) = \frac{\varphi_l}{s + \psi_l}, \quad (21)$$

where s is the Laplace variable; φ_l and ψ_l are the uncertainty parameters (gain and pole), subject to the limits that are defined according to the values of the hydraulic subsystems parameters, as shown in the appendix. These limits can be written as:

$$\varphi_{\min} < \varphi_l \leq \varphi_{\max}, \quad \psi_{\min} \leq \psi_l \leq \psi_{\max}. \quad (22)$$

The H-infinity mixed-sensitivity method was chosen to synthesize a robust control law $v(s) = C_{F_h}(s) \tilde{F}_h(s)$, where $C_{F_h}(s)$ is the controller TF and $\tilde{F}_h(s)$ is the hydraulic force tracking error, to handle the parameters uncertainties. The method applied is based on the formatting of sensitivity (S) and complementary sensitivity (T) TFs, which are given by (Skogestad and Postlethwaite, 2005):

$$S(s) = \frac{1}{1 + L(s)}, \quad T(s) = \frac{L(s)}{1 + L(s)}, \quad (23)$$

with $L(s) = C_{F_h}(s) G_{F_h}(s)$ as the loop TF. The requirements of performance and robustness to the controller synthesis are captured with the following weighting functions (Skogestad and Postlethwaite, 2005):

$$W_S(s) = \frac{s/M_S + \omega_S}{s + \omega_S \varepsilon_S} \Rightarrow |W_S S| \leq \gamma, \quad W_T(s) = \frac{s + \omega_T/M_T}{\varepsilon_T s + \omega_T} \Rightarrow |W_T T| \leq \gamma, \quad \forall \omega, \quad (24)$$

where $M_{S,T}$, $\omega_{S,T}$ and $\varepsilon_{S,T}$ are the weighting functions parameters chosen according to the design requirements and $\gamma \in \mathfrak{R}$ is a scalar. The first-order weighting functions were chosen to enable the structured synthesis of the H-infinity compensation term as a PI controller.

To facilitate the practical implementation of the H-infinity term, the controller $C_{F_h}(s)$ was synthesized through the structured approach available in the MATLAB®, considering a PI structure for the controller as shown below:

$$C_{F_h}(s) = \frac{k_p s + k_i}{s}, \quad (25)$$

with k_p and k_i as the proportional and integral control gains of the hydraulic subsystem, respectively. The controller TF obtained for each actuator can be put into the matrix $\mathbf{C}_\infty(s) = \text{diag}[C_{F_{h1}}(s), \dots, C_{F_{h4}}(s)]$. Hence, the control term \mathbf{v} can be written as: $\mathbf{v} = -\mathbf{C}_\infty \tilde{\mathbf{F}}_h$ where $\tilde{\mathbf{F}}_h \in \mathfrak{R}^4$ is the vector of tracking errors of the hydraulic forces, that is given by: $\tilde{\mathbf{F}}_h = \mathbf{F}_h - \mathbf{F}_{hd}$, with $\mathbf{F}_{hd} \in \mathfrak{R}^4$ as the vector of desired hydraulic forces.

Manipulator controller

As shown in Slotine and Li (1991), the direct implementation of the proposed cascade controller can cause a high-frequency activity in the control signals. This phenomenon is called “chattering” and is characterized by the “excess” of the control activity generated by the $\text{sign}(\bullet)$ terms in the control laws when system states reach the sliding surface (Slotine and Li, 1991). This type of control activity can make the system unstable and compromise the system actuators prematurely (Nguyen, 2000). Thus, to reduce the chattering problem, the $\text{sign}(\bullet)$ can be smoothed by its approximation with a sigmoidal function. In this work, the function $\tanh(\bullet)$ approximated the $\text{sign}(\bullet)$. Therefore, the equations of the cascade controller can be rewritten as:

$$\dot{\tilde{\omega}} = \hat{\mathbf{M}}^{-1}(\mathbf{F}_h - \hat{\mathbf{G}}) + \hat{\Phi} - \mathbf{L}\tilde{\omega}, \quad (26)$$

$$\dot{\hat{\Phi}} = -\Gamma \tanh(\mathbf{E}\tilde{\omega}), \quad (27)$$

$$\mathbf{F}_{hd} = \hat{\mathbf{M}} \left[\ddot{\mathbf{q}}_r - \mathbf{Z} \tanh(\mathbf{F}\mathbf{s}) - \mathbf{K}\mathbf{s} - \hat{\Phi} \right] + \hat{\mathbf{G}}, \quad (28)$$

$$\mathbf{u}_v = (\mathbf{A}_a \hat{\mathbf{E}}_l)^{-1} (\mathbf{A}_a \hat{\mathbf{F}}_l \mathbf{J}^T \dot{\mathbf{q}} - \mathbf{C}_\infty \tilde{\mathbf{F}}_h), \quad (29)$$

where $\mathbf{E} = \text{diag}[1/e_1, \dots, 1/e_4]$, with $0 < e_i \leq 1$, and $\mathbf{F} = \text{diag}[1/f_1, \dots, 1/f_4]$, with $0 < f_i \leq 1$, are gain matrices used to regulate the smoothing of the $\tanh(\bullet)$ approximation.

The direct implementation of the control law of the hydraulic subsystem will result in an algebraic loop because the matrix $\hat{\mathbf{E}}_l$ is a function of the sign of \mathbf{u}_v , as shown in the appendix. However, this problem can be circumvented with the assumption that there is no reverse flow in the hydraulic subsystem, thus, $\hat{\mathbf{E}}_l$ will be positive definite and, as shown in Santos (2001), the sign of \mathbf{u}_v will be equal to the sign of $\mathbf{A}_a \hat{\mathbf{F}}_l \mathbf{J}^T \dot{\mathbf{q}} - \mathbf{C}_\infty \tilde{\mathbf{F}}_h$. Therefore, to the calculation of $\hat{\mathbf{E}}_l$, the vector \mathbf{u}^* is defined as follows: $\mathbf{u}^* \triangleq \mathbf{A}_a \hat{\mathbf{F}}_l \mathbf{J}^T \dot{\mathbf{q}} - \mathbf{C}_\infty \tilde{\mathbf{F}}_h$, with $\text{sign}(\mathbf{u}_v) = \text{sign}(\mathbf{u}^*)$.

RESULTS

In this section, the results from the manipulator simulation with the control are presented. Figure 4 shows the desired trajectory (built with cycloidal functions) in the workspace used to represent a complete operation composed by digging and dump tasks. This trajectory is composed of nine (9) phases which are often used in real applications. The reference model with the proposed cascade controller was simulated through the numerical integration of its differential equations in MATLAB/Simulink© environment. The time integration was performed with the ODE4 (solver based in the 4th order Runge-Kutta method) with fixed step (0,001 seconds). Measurement noise (additive white Gaussian noise) was added in the state variables to replicate the operating conditions (see the appendix). The model parameters used in the simulation are found in de Oliveira and Donha (2018) and the values of the controller gains are shown in the appendix.

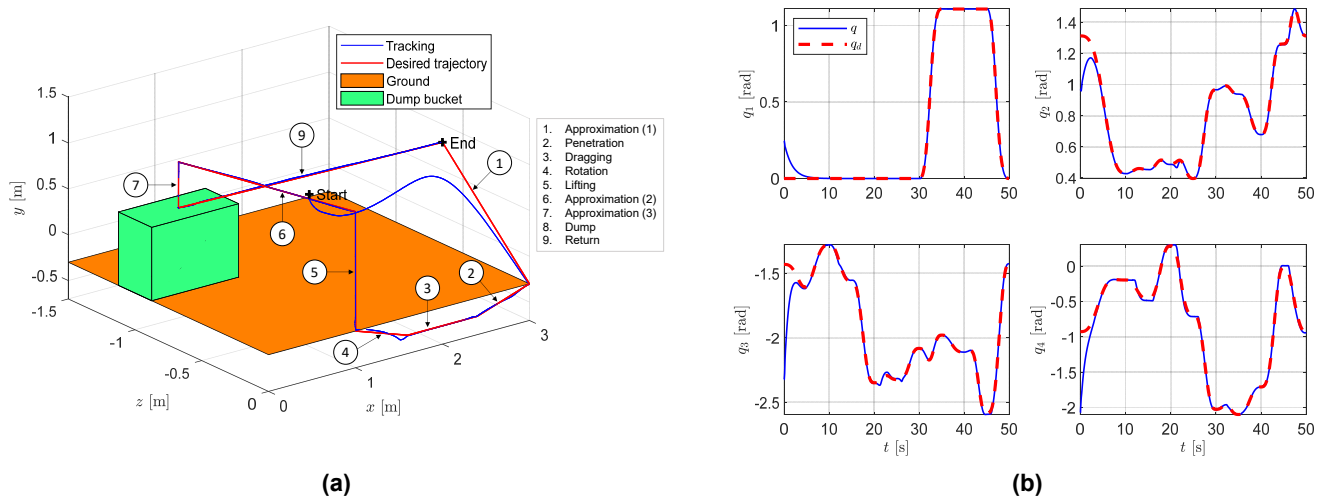


Figure 4 – Comparative trajectory tracking. (a) Workspace. (b) Joints space.

The comparison between the desired and obtained trajectory are also shown in Fig. 4 (workspace and joints space). In Figure 5 is shown the time history of others results (states’ convergence, disturbances estimation, control signals and hydraulic forces). Analyzing the Fig. 4, it is noted that the cascade controller gives a good tracking in the workspace and in the joints space during all the operation. And, as seen in the Fig. 5, the proposed controller ensures the states

convergence to the sliding surface in finite time. The SMDO gives a good estimative of the disturbances. The generated control signals are acceptable (low chattering) and stay within the saturation limits. In addition, the generated hydraulic forces replicate the observations made with the control signals.

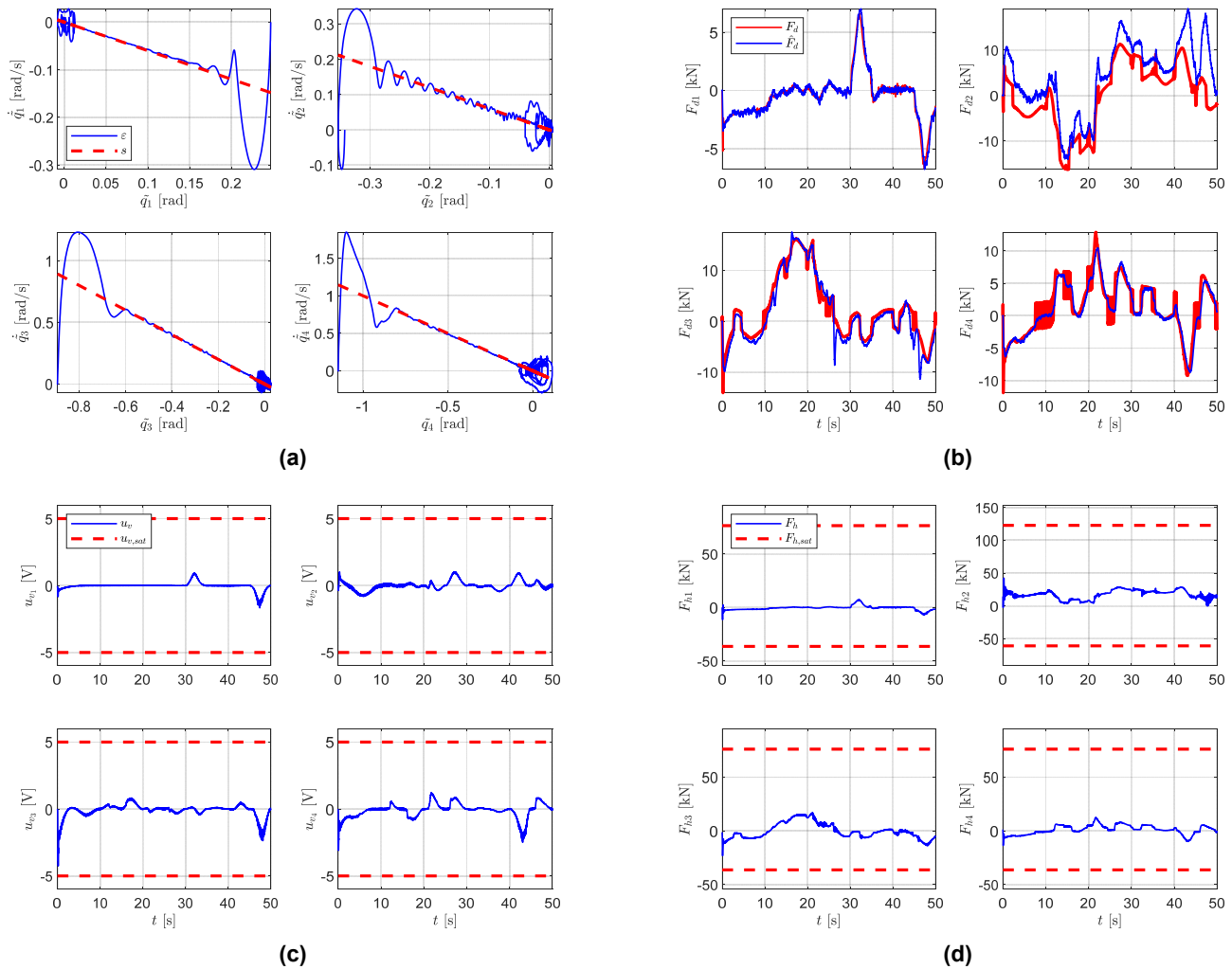


Figure 5 – Results. (a) States’ convergence. (b) Disturbances estimation. (c) Control signals. (d) Hydraulic forces.

Based on the simulations results, it is verified that the proposed control can handle to the disturbances, uncertainties and the modeling errors (task efforts, friction forces, leakage flow, bulk modulus variation, model simplifications and measurements noises) during a complete operation while keeping a good tracking of the desired trajectory.

CONCLUSIONS

In this work, a controller for the manipulator of a mini-excavator was developed. The controller is divided into two control laws, one for the mechanical subsystem and the other for the hydraulic one. The control law for the mechanical subsystem is based on SMC technic, and the hydraulic subsystem control law is composed of a feedback linearization with an H-infinity compensation term. The developed controller was simulated with a reference model in a complete operation, involving digging and dump tasks. Good tracking was achieved in the workspace and in the joints space. This may indicate the applicability of the proposed controller for the equipment automation. For future works, the controller will be tested in a real system.

REFERENCES

- Fales, R., 2004, “Robust Control Design for an Electrohydraulic Wheel Loader System with a Human-In-The-Loop Assessment in a Virtual Environment”, Ph.D. Thesis, Iowa State University, Iowa, 131 p.
- He, Q. et al., 2006, “Modeling and control of hydraulic excavator’s arm”, Journal of Central South University of Technology, Vol.13, No. 4, pp. 422-427.
- Hoan, L.Q. et al., 2011, “Study on Modeling and Control of Excavator”, International Journal of Project Management, Vol.28, No. 3, pp. 969-974.

- Koivo, A.J. et al., “Modeling and Control of Excavator Dynamics during Digging Operation”, Journal of Aerospace Engineering, Vol.9, No. 1, pp. 10-18.
- MathWorks, 2018, “Hydraulic capacity of constant volume – MATLAB”. Available in: <<https://www.mathworks.com/help/physmod/simscape/ref/constantvolumehydraulicchamber.html>>.
- Merrit, H., 1967, “Hydraulic Control Systems”, John Wiley & Sons, New York, 358 p.
- Nguyen, Q.H., 2000, “Robust Low-Level Control of Robotic Excavation”, Ph.D. thesis, University of Sydney, Sydney, 234 p.
- de Oliveira, É.L., Donha, D.C., 2017, “Dynamic Modelling of the Manipulator of a Mini Hydraulic Excavator in Load Condition”, DINAME 2017, São Sebastião, São Paulo, 10 p.
- de Oliveira, É.L., Donha, D.C., 2018, “Modelling of the Manipulator of a Mini Hydraulic Excavator”, Proceedings of DINAME 2017, Lecture Notes in Mechanical Engineering, Springer, pp 305-318.
- Santos, C.H., 2001, “Modeling and Cascade Control of a Hydraulic Manipulator”, M.Sc. Thesis, Federal University of Santa Catarina, Santa Catarina, 124 p.
- Skogestad, S., Postlethwaite, I., 2005, “Multivariable Feedback Control”, John Wiley & Sons, New York, 574 p.
- Slotine, J.-J. E.; Li, W., 1991, “Applied Nonlinear Control”, Prentice Hall, New Jersey, 461 p.
- Valdiero, A.C., 2005, “Control of Hydraulic Robots with Friction Compensation”, Ph.D. Thesis, Federal University of Santa Catarina, Santa Catarina, 177 p.

RESPONSIBILITY NOTICE

The authors are the only responsible for the printed material included in this paper.

APPENDIX

Friction force

The friction force model of the cylinders is given by (de Oliveira and Donha, 2018):

$$F_f = F_C \left[1 + (K_{\text{static}} - 1) \exp(-c_v |v_c|) \right] \text{sign}(v_c) + B_v v_c, \quad (30)$$

with F_C as the Coulomb friction force, K_{static} as the coefficient of static friction, c_v as the coefficient of transition velocity, B_v as the coefficient of viscous friction and v_v as the linear velocity of the cylinder.

Task efforts

The digging force model used was originally adopted by Koivo et al. (1996) to the application in the dynamic model of a hydraulic excavator. Nguyen (2000) applied the same model in a robotic excavator as follows:

$$F_{\text{digging}} = k_s b h, \quad (31)$$

where k_s is the specific resistance to soil cut, b and h are, respectively, the width and thickness of the soil slice. The width and thickness used in the simulation are: $b = 0,41$ (m) and $h_{\text{max}} = 0,20$ (m).

The dump force is calculated based on the maximum volumetric capacity of the bucket (according to the norm SAE J296 for mini-excavators) as shown below (de Oliveira and Donha, 2017):

$$F_{\text{dump}} = \rho_s V_s g, \quad (32)$$

with ρ_s as the soil density, V_s as the heap volume and g as the gravity acceleration.

Sandy-loam was considered as the soil type and its parameters can be found in Koivo et al. (1996), Nguyen (2000) and in de Oliveira and Donha (2017).

The forces were introduced in the mechanical subsystem model as active forces, as shown in Nguyen (2000) and in de Oliveira and Donha (2017).

Hydraulic subsystem

The terms of the hydraulic subsystem model for $i = 1, \dots, n_{\text{cylinders}}$ are giving by:

$$\mathbf{E}_a(\mathbf{q}, \mathbf{p}_a, \mathbf{x}_v) = \text{diag} \left[\frac{\beta(p_{ai})}{V_{ai}(q_i)} k_{ai} g_{ai}(p_{ai}, x_{vi}) \right], \quad \mathbf{E}_b(\mathbf{q}, \mathbf{p}_b, \mathbf{x}_v) = \text{diag} \left[\frac{\beta(p_{bi})}{V_{bi}(q_i)} k_{bi} g_{bi}(p_{bi}, x_{vi}) \right], \quad (33)$$

$$\mathbf{F}_a(\mathbf{q}) = \text{diag} \left[\frac{\beta(p_{ai})}{V_{ai}(q_i)} A_{ai} \right], \mathbf{F}_b(\mathbf{q}) = \text{diag} \left[\frac{\beta(p_{bi})}{V_{bi}(q_i)} A_{bi} \right], \mathbf{D}_a(\mathbf{q}) = \text{diag} \left[\frac{\beta(p_{ai})}{V_{ai}(q_i)} \right], \mathbf{D}_b(\mathbf{q}) = \text{diag} \left[\frac{\beta(p_{bi})}{V_{bi}(q_i)} \right], \quad (34)$$

where β is the bulk modulus, $V_{ai} = A_{ai}(\tilde{l}_{ai} + \bar{l}_{CiHi}) + V_{ppi}$ is the volume of the chamber ai , $V_{bi} = A_{bi}(\tilde{l}_{bi} - \bar{l}_{CiHi}) + V_{ppi}$ is the volume of the chamber bi , with $\tilde{l}_{ai,bi} = l_{ai,bi}(q_i(t_0))$ and $A_{ai,bi}$ as the initials (in time t_0) lengths and the cross-section areas of these chambers, respectively; V_{ppi} is the fluid volume inside the pipelines and \bar{l}_{CiHi} is the cylinder displacement, that is given by: $\bar{l}_{CiHi} = l_{CiHi} - \bar{l}_{CiHi}$, with $l_{CiHi} = l_{CiHi}(q_i)$ as the cylinder length and $\bar{l}_{CiHi} = l_{CiHi}(q_i(t_0))$ as its initial length; k_{ai} and k_{bi} are the flow rate coefficients of ports ai and bi of the valve (when the dynamics of the valve is not negligible); g_{ai} and g_{bi} are nonlinear functions used to describe the flow rates through the orifices of the valve as follows:

$$g_{ai}(p_{ai}, u_{vi}) = \begin{cases} \sqrt{|p_s - p_{ai}|} \text{sign}(p_s - p_{ai}) & \text{if } u_{vi} \geq 0 \\ \sqrt{|p_{ai} - p_r|} \text{sign}(p_{ai} - p_r) & \text{if } u_{vi} < 0 \end{cases}, g_{bi}(p_{bi}, u_{vi}) = \begin{cases} \sqrt{|p_{bi} - p_r|} \text{sign}(p_{bi} - p_r) & \text{if } u_{vi} \geq 0 \\ \sqrt{|p_s - p_{bi}|} \text{sign}(p_s - p_{bi}) & \text{if } u_{vi} < 0 \end{cases}, \quad (35)$$

with p_s as the supply pressure, p_r as the return pressure, p_{ai} as the pressure of the chamber ai , p_{bi} as the pressure of the chamber bi and u_{vi} as the control signal.

The bulk modulus (β) is calculated with the semi-empirical model presented in MathWorks (2018). This model expresses the bulk modulus as a function of the chambers' pressures.

The terms of the hydraulic subsystem reduced model are shown below:

$$\hat{\mathbf{E}}_l(\mathbf{q}, \mathbf{F}_h, \mathbf{u}_v) = \text{diag} \left[\frac{\beta_e}{V_{ai}(q_i)} \left(1 + \frac{\alpha_{ci}^2}{r_{vi}} \right) K_{li} g_{li}(F_{hi}, u_{vi}) \right], \quad (36)$$

$$\hat{\mathbf{F}}_l(\mathbf{q}) = \text{diag} \left[\frac{\beta_e}{V_{ai}(q_i)} \left(1 + \frac{\alpha_{ci}^2}{r_{vi}} \right) A_{ai} \right], \hat{\mathbf{D}}_l(\mathbf{q}) = \text{diag} \left[\frac{\beta_e}{V_{ai}(q_i)} \left(1 + \frac{\alpha_{ci}}{r_{vi}} \right) \right], \quad (37)$$

where β_e is the effective value of the bulk modulus, $r_{vi} = V_{bi} / V_{ai}$ is the ratio between the volume of the chambers ai and bi , $\alpha_{ci} = A_{bi} / A_{ai}$ is the ratio between the cross-section areas of these chambers and $K_{li} = (\sigma_{vi} K_{ai}) / \sqrt{\sigma_{vi}^2 + \alpha_{ci}^3}$ is the coefficient of load flow rate, with $\sigma_{vi} = K_{bi} / K_{ai}$ as the ratio between the flow rates coefficients of the valve, where K_{ai} and K_{bi} are the hydraulic constants of ports ai and bi of the valve (when the dynamics of the valve is negligible) and g_{li} is a nonlinear function used to describe the load flow rate as follows:

$$g_{li}(F_{hi}, u_{vi}) = \begin{cases} \sqrt{|p_s - F_{hi}/A_{ai} - \alpha_{ci} p_r|} \text{sign}(p_s - F_{hi}/A_{ai} - \alpha_{ci} p_r) & \text{if } u_{vi} \geq 0 \\ \sqrt{|\alpha_{ci} p_s + F_{hi}/A_{ai} - p_r|} \text{sign}(\alpha_{ci} p_s + F_{hi}/A_{ai} - p_r) & \text{if } u_{vi} < 0 \end{cases}, \quad (38)$$

with F_{hi} as the hydraulic force. In Eq. (38), the term F_{hi}/A_{ai} comes from the relation between hydraulic force and load pressure, that is given by: $F_{hi} = A_{ai} p_{li}$, where p_{li} is the load pressure.

Cascade Control

The gains used in the simulation are shown below:

$$\mathbf{\Lambda} = \text{diag}[0, 6; 0, 6; 1, 0; 1, 0], \mathbf{K} = \text{diag}[50; 100; 625; 1125], \mathbf{Z} = \text{diag}[250; 500; 3125; 5625], \quad (39)$$

$$\mathbf{\Gamma} = \text{diag}[250; 500; 850; 850], \mathbf{L} = \text{diag}[150; 300; 525; 525], e_i = 1, f_i = 0, 30, k_p = 4, 40, k_i = 6, 60.$$

The limits of the uncertain parameters in the hydraulic force TF are given by:

$$0 < \varphi_{li} \leq 1, \frac{\beta_e}{V_{ai, \max}} \left(1 + \frac{\alpha_{ci}}{r_{vi, \min}} \right) C_{li} \leq \psi_{li} \leq \frac{\beta_e}{V_{ai, \min}} \left(1 + \frac{\alpha_{ci}}{r_{vi, \max}} \right) C_{li}, \quad (40)$$

where $C_{li} = C_{ini} (\sigma_{vi}^2 + \alpha_{ci}^2) / (\sigma_{vi}^2 + \alpha_{ci}^3)$ is the load pressure leakage coefficient, with C_{ini} as the leakage coefficient.

The weighting functions parameters used are: $M_S = 2$, $M_T = 1, 15$, $\omega_S = 3$ (rad/s), $\omega_T = 5$ (rad/s), $\varepsilon_S = 1 \cdot 10^{-3}$ and $\varepsilon_T = 1 \cdot 10^{-6}$. With these parameters was obtained an H-infinity controller with $\gamma \cong 1, 20$.

The noises' covariance considered in the simulation are: $\sigma_{q_i}^2 = 1 \cdot 10^{-6}$, $\sigma_{\dot{q}_i}^2 = 1, 23 \cdot 10^{-5}$ and $\sigma_{F_{hi}}^2 = 1, 3 \cdot 10^7$.